Nuclear Inst. and Methods in Physics Research, A 978 (2020) 164395

Contents lists available at ScienceDirect

Nuclear Inst. and Methods in Physics Research, A

journal homepage: www.elsevier.com/locate/nima

First demonstration of real-time in-situ dosimetry of X-ray microbeams using a large format CMOS sensor

Samuel Flynn [a,b,*], Tony Price [a,b], Philip P. Allport [a], Ileana Silvestre Patallo [b,c], Russell Thomas [b], Anna Subiel [b], Stefan Bartzsch [d,e], Franziska Treibel [e], Mabroor Ahmed [e], Jon Jacobs-Headspith [f], Tim Edwards [f], Isaac Jones [f], Dan Cathie [f], Nicola Guerrini [g], Iain Sedgwick [g]

[a] School of Physics and Astronomy, University of Birmingham, Birmingham, United Kingdom
[b] Medical Physics, National Physical Laboratory, Teddington, United Kingdom
[c] UCL Cancer Institute, University College London, London, United Kingdom
[d] Helmholtz Centre Munich, Institute for Radiation Medicine, Munich, Germany
[e] Technical University of Munich, School of Medicine, Klinikumrechtsder Isar, Department of Radiation Oncology, Munich, Germany
[f] vivaMOS Ltd, Southampton, United Kingdom
[g] Rutherford Appleton Laboratory, Oxford, United Kingdom

ARTICLE INFO

MSC:
00-01
99-00

Keywords:
CMOS
Microbeam
Radiotherapy
Dosimetry

ABSTRACT

Microbeam radiotherapy is a novel type of radiotherapy in which narrow beams of radiation (typically less than 500 μm) are spatially fractionated, delivering a non-uniform distribution to the target tumour volume. Due to the very high dose gradients and very small beams involved, new dosimetric techniques are required for translation into clinical practise. Current real-time beam monitoring is typically performed using 1 dimensional silicon strip detectors or wire chambers, with 2D beam information measured offline using radiochromic film (requiring a minimum of 24 h to self-develop).

Using an Xstrahl SARRP X-ray irradiation device with a bespoke microbeam collimator at the Technical University of Munich, Germany, the newly developed vM1212 detector was exposed to a variety of microbeams (220 kV, nominal slit widths 0–100 μm) for evaluation of in vivo real time verification.

The performance of the detector was assessed by changing the collimator slit width (and thus microbeam FWHM) mid-irradiation. Microbeam FWHMs of 130–190 μm could be measured in this manner in addition to temporally monitoring other basic parameters such as the radiation intensity. More advanced parameters could be calculated as the tungsten slits within the microbeam collimator opened and closed such as the rate of change of FWHM; the peak–valley-dose-ratio (PVDR); and the sub-pixel movement of each microbeam peak.

This work demonstrates the potential of radiation hard CMOS sensors in radiotherapy for in vivo real-time monitoring of X-ray microbeams FWHM, intensity and position.

1. Introduction

Microbeam radiotherapy (MRT) is a novel type of external radiation treatment, in which the radiation field is spatially fractionated into narrow beams (typically less than 100 μm), delivering a non-uniform distribution to the target tumour volume [1]. Preclinical studies have indicated that despite the fact that not all the tumour cells receive a lethal dose, MRT produces greater efficacy for tumour control than traditional uniform radiation fields (with the same level of normal tissue sparing) [2], an effect attributed to preferential tumour vascular damage [3] and radiation-induced bystander and abscopal effects [4]. Together, these outcomes suggest that MRT could be used to treat radio-resistant tumours that are currently incurable [5]. Due to the very high dose gradients and small beams involved, new dosimetric techniques are required for translation into clinical practise.

Currently, dosimetric measurements of MRT are typically performed using very small volume ionisation chambers, solid state detectors, or radiochromic film; however these are unsuitable for real-time in-situ dosimetry (with radiochromic films requiring a minimum of 24 h to self-develop). One dimensional silicon strip detectors have been used with success [6], however they cannot provide 2D profiles of the radiation field and will be sensitive to angular misalignment.

An annotated diagram of a few of the microbeam parameters is shown in Fig. 1, where the full width at half maximum (FWHM) and peak to peak separation are labelled. The commonly quoted parameter peak-to-valley-dose-ratio (PVDR) is calculated as a ratio of the peak

* Corresponding author at: School of Physics and Astronomy, University of Birmingham, Birmingham, United Kingdom.
E-mail address: sam.flynn@npl.co.uk (S. Flynn).

https://doi.org/10.1016/j.nima.2020.164395
Received 29 February 2020; Received in revised form 1 May 2020; Accepted 29 May 2020
Available online 18 July 2020
0168-9002/

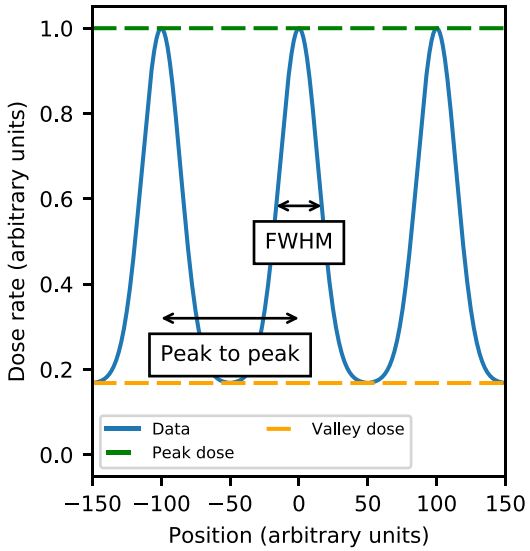

Fig. 1. Annotated diagram of microbeam profile features.

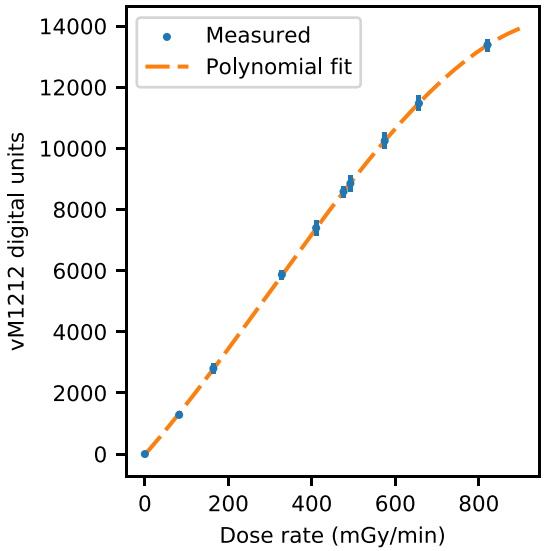

Fig. 2. Calibration curve of the vM1212 detector. Uncertainties shown are one standard deviation.

dose and the valley dose. It has been shown in preclinical studies that varying each of these parameters impacts the treatment outcome and a large amount of research is still ongoing to optimise these parameters [7–10].

The suitability of large format CMOS (complementary metal–oxide–semiconductor) sensors for microbeam dosimetry was first evaluated by Flynn et al. [11], where small field's 2D dose distributions acquired with the vM1212 detector (based on the LASSENA pixel design [12]) were compared to EBT3 radiochromic film (scanned with two detection methods). Whilst agreement was found between the two methods, the investigation was limited in scope to microbeams of fixed width averaged over several minutes of exposure, due to the dose levels required with the radiochromic film.

In this investigation we evaluated and analysed individual frames acquired by the vM1212 detector for X-ray microbeams with static and changing FWHM to determine the potential suitability for in vivo or in-situ monitoring of microbeam deliveries with large format CMOS detectors.

2. Method

A vM1212 detector, a large format CMOS sensor with 50 μm pixel pitch and approximately 6 x 6 cm^2 active area, was placed in a Small Animal Radiation Research Platform (SARRP) installed at the Technical University of Munich. A custom designed Tungsten X-ray microbeam collimator with fifty-one 100 μm wide slits [13], based on the design by Bartzsch et al. [14], was installed within the X-ray cabinet and was used to shape the microbeams. The collimator consisted of three layers of tungsten, with the middle layer connected to two piezoelectric actuators, which were controlled via software. By aligning the middle layer, nominal slit widths of 0-100 μm were achievable.

The detector was placed at a distance of 29 cm from the X-ray source, and 6.8 cm below the microbeam collimator. 1 cm of water equivalent bolus was placed on top of the vM1212 detector and used as build-up material to imitate build-up tissue conditions in animal preclinical irradiations.

The response of the vM1212 detector was calibrated within the SARRP (with an open field, chamber at SSD (Source Surface Distance) 33 cm, 2 cm depth in water and 5 cm backscatter material) against a PTW 30012 ionisation chamber, which was traceable to the National Physical Laboratory primary standard for medium energy X-rays. A consistent integration time of 28 ms was selected on the vM1212 detector. For the investigation, the SARRP fine focus was selected, and the sensor was irradiated with 220 kV X-rays at the maximum beam current of 2.9 mA. The penetration quality of the beam defined by the half value layer (HVL) was measured to be 0.68 mm Cu. HVL represents the thickness of a material (in mm) that attenuates the intensity of the beam by 50%.

Temperature, pressure and relative humidity were recorded throughout the investigation to check for consistency but no additional corrections to the vM1212 detector were made. Due to the limitations of the low-performance laptop running the software to acquire the images from the detector, a maximum of 140 frames could be taken consecutively representing approximately 4 s of data.

Evaluation of the detector's performance was achieved by changing the nominal width of the microbeam slits. Using the bespoke software to control the actuators, the nominal slit width was changed from 0 to 100 μm as fast as it was able to. A measurement of the average dose rate for a variety of nominal slit widths was carried out (with 140 frames). Microbeam parameters for each of the peaks were fitted with a Python script using the SciPy module [15], assuming each peak was a perfect Gaussian with an offset. Associated uncertainties were calculated by comparing calculated parameters for the fitted microbeam peaks, with peaks rejected if the FWHM was determined to be greater than a non-physically possible 300 μm width. In addition to stationary beams, the vM1212 detector was set to record while the nominal slit width dynamically changed.

3. Results

The calibration curve of the vM1212 detector is shown in Fig. 2, after subtraction of a dark current. Although the response of the vM1212 detector was found to be linear within the dose rate range used, a third order polynomial was applied to the signal from the vM1212 detector.

It was found that the vM1212 detector was able to obtain the full microbeam profile with an adequate level of discrimination between the low dose "valleys" and the high "peaks" regions for a single frame acquisition of static beams (Fig. 3). As reported by Flynn et al. [11]. the produced microbeams were found to be larger than the nominal slit width, attributed to the finite size of the X-ray source (400 μm). The central three peaks for the different nominal slit widths are shown in Fig. 4, where the centre of each peak is observed to move in the positive x direction as the nominal slit width decreases.

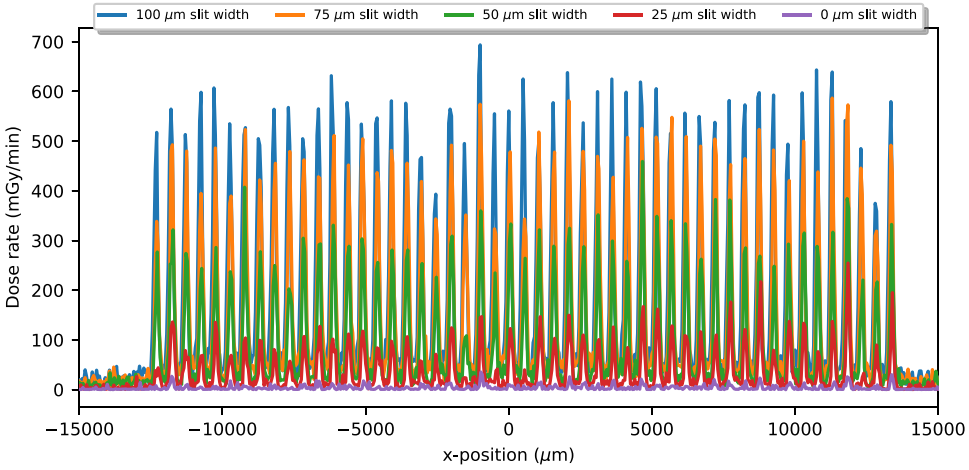

Fig. 3. Comparison of microbeam nominal slit widths acquired in single frames by the vM1212 detector.

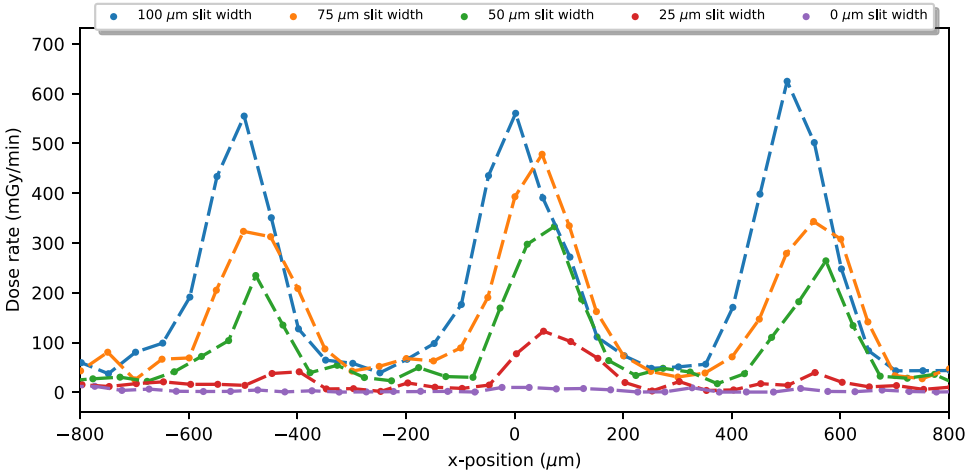

Fig. 4. Comparison of the central microbeam peaks acquired in single frames by the vM1212 detector.

As shown in Fig. 5, by using the calibrated response of the vM1212 detector, it was found that the mean dose rate (averaged within the ±15 mm region shown on Fig. 3 for all of the 140 frames obtained at each nominal slit width) did not vary linearly with nominal slit width. This is likely due to complex scattering effects within the collimator. The coefficient of variation (defined as the standard deviation divided by the mean) rapidly increased for decreasing nominal slit width, indicating a larger variation between frames. As the X-ray source has not changed, this increase in variability in the intensity is likely due to photon shot noise.

Fig. 6 shows the variation of the investigated parameters during the recorded time while the nominal slit width was dynamically increased. The mean FWHM, as expected, was found to linearly increase, with a decrease in the FWHM standard deviation at larger nominal slit widths.

The PVDR remained approximately constant as the nominal slit width increased, with a smaller standard deviation for larger nominal slit widths. In Flynn et al. [11] it was observed that the PVDR measured by the vM1212 detector for static measurements remained approximately constant between 25 and 100 μm, decreasing from approximately 14 at 25 μm to 4 at 0 μm. Due to the limited amount of data acquired for a moving slit, dynamic slit widths below 15 μm were not able to be observed.

The peak to peak separation was observed to be approximately constant above 30 μm, before which point the mean value and its standard deviation increased. As the physical separation of the microbeam slits did not change (only their widths), this increase in calculated peak to

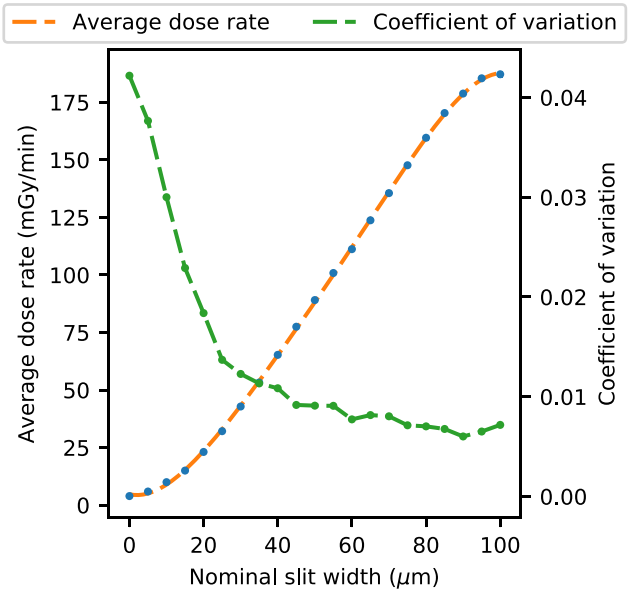

Fig. 5. Average dose rate and coefficient of variation (standard deviation/mean) of the microbeam field for various nominal slit widths.

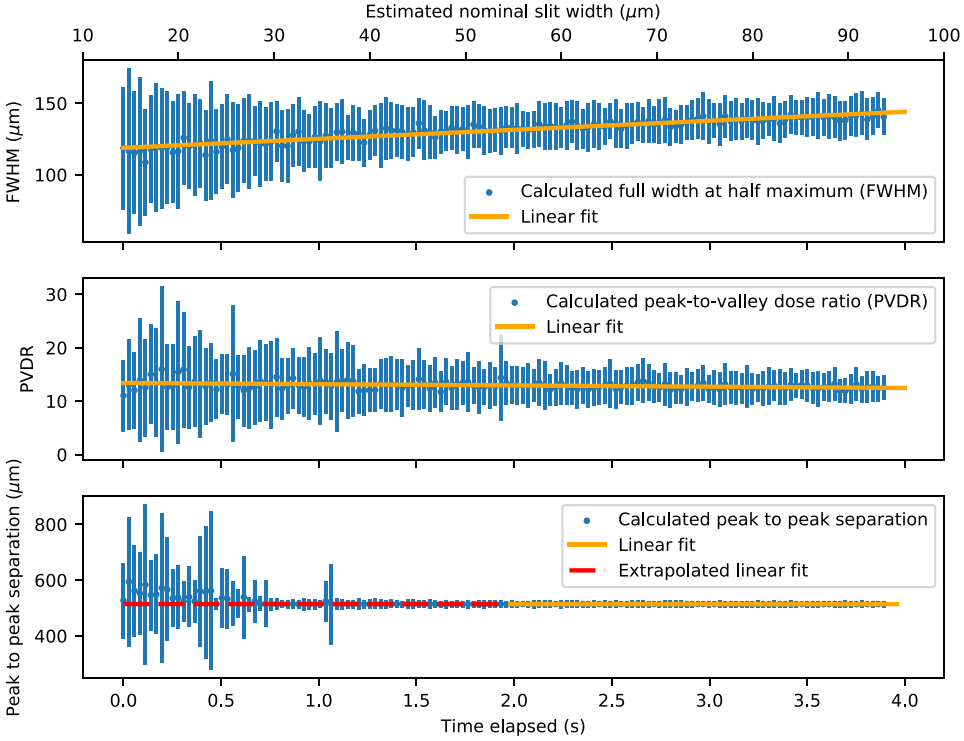

Fig. 6. Calculated parameters of the X-ray microbeam field as the nominal slit width increased (one standard deviation shown).

peak separation at low nominal slit widths is likely to be a consequence of the low intensity signal that was being recorded by the vM1212 detector.

4. Discussion

As shown in Fig. 6 the uncertainty of all calculated parameters increases with decreasing nominal slit width, limiting potential pre-clinical impact of the vM1212 detector where slit widths of 25–50 μm are common. It is likely that photon shot noise contributes a significant source of uncertainty for low intensity signals. For in vivo monitoring this could be minimised by performing a moving average on several frames.

It is possible that the integration time of the detector could be automatically increased to compensate for poor signal, but this is beyond the scope of this investigation. In addition, it is possible that other methods for determining these parameters may be more suitable such an auto-correlation function or fast-Fourier transform to determine the peak to peak separation, rather than relying heavily on fitted Gaussian profiles. The peak fitting function could also be improved, with more peaks that are not physically possible being rejected. This would likely have an effect of reducing the size of the standard deviations shown in Fig. 6.

Due to the limits of the electronic controller of the piezoelectric actuators that determine the nominal slit width, rapidly changing between several prescribed FWHMs for evaluation with the vM1212 detector was not possible. This is however, an area of interest for future research, as real-time verification of microbeam radiotherapy could be developed into a treatment control package.

5. Conclusion

The results of this work demonstrate the feasibility of CMOS sensors for in-situ verification of microbeam X-ray irradiations. The vM1212 detector allowed for real time determination of beam position and shape which could be built into a future microbeam treatment planning system. Further research is still required to develop future CMOS sensors with radiation tolerance in excess of 20 Mrad, higher frame rate for faster in vivo monitoring, smaller pixel pitch for greater spatial resolution, and with larger dynamic range to enable measurements of larger peak to valley dose ratio microbeams.

Declaration of competing interest

Due to the prototype nature of the device, the manufacturer of the vM1212 detector, vivaMOS Ltd, has been involved in data collection providing advice and technical support throughout the investigation.

Acknowledgements

This work was supported by the Science and Technology Facilities Council, United Kingdom (grant ST/P002552/1) and by the UK government's Department for Business, Energy and Industrial Strategy.

References

[1] D.N. Slatkin, P. Spanne, F.A. Dilmanian, M. Sandborg, Microbeam radiation therapy, Med. Phys. 19 (6) (1992) 1395–1400, http://dx.doi.org/10.1118/1.596771.

[2] A. Bouchet, R. Serduc, J.A. Laissue, V. Djonov, Effects of microbeam radiation therapy on normal and tumoral blood vessels, Phys. Medica 31 (6) (2015) 634–641, http://dx.doi.org/10.1016/J.EJMP.2015.04.014.

[3] R. Serduc, et al., Brain tumor vessel response to synchrotron microbeam radiation therapy: a short-term *in vivo* study, Phys. Med. Biol. 53 (13) (2008) 3609–3622, http://dx.doi.org/10.1088/0031-9155/53/13/015.

[4] E. Bräuer-Krisch, et al., Effects of pulsed, spatially fractionated, microscopic synchrotron X-ray beams on normal and tumoral brain tissue, Mutat. Res. - Rev. Mutat. Res. 704 (1–3) (2010) 160–166, http://dx.doi.org/10.1016/j.mrrev.2009.12.003.

[5] F.A. Dilmanian, et al., Response of rat intracranial 9L gliosarcoma to microbeam radiation therapy, Neuro Oncol. 4 (1) (2002) 26–38, http://dx.doi.org/10.1093/neuonc/4.1.26.

[6] M. Povoli, et al., Thin silicon strip detectors for beam monitoring in Micro-beam Radiation Therapy, J. Instrum. 10 (11) (2015) P11007, http://dx.doi.org/10.1088/1748-0221/10/11/P11007.

[7] R. Serduc, et al., Synchrotron microbeam radiation therapy for rat brain tumor palliation—influence of the microbeam width at constant valley dose, Phys. Med. Biol. 54 (21) (2009) 6711–6724, http://dx.doi.org/10.1088/0031-9155/54/21/017.

[8] E. Bräuer-Krisch, et al., Medical physics aspects of the synchrotron radiation therapies: Microbeam radiation therapy (MRT) and synchrotron stereotactic radiotherapy (SSRT), Phys. Medica 31 (6) (2015) 568–583, http://dx.doi.org/10.1016/J.EJMP.2015.04.016.

[9] N. Annabell, N. Yagi, K. Umetani, C. Wong, M. Geso, Evaluating the peak-to-valley dose ratio of synchrotron microbeams using PRESAGE fluorescence, J. Synchrotron Radiat. (2012) http://dx.doi.org/10.1107/S0909049512005237.

[10] P. Regnard, et al., Irradiation of intracerebral 9l gliosarcoma by a single array of microplanar x-ray beams from a synchrotron: Balance between curing and sparing, Phys. Med. Biol. 53 (4) (2008) 861–878, http://dx.doi.org/10.1088/0031-9155/53/4/003.

[11] S. Flynn, et al., Evaluation of a pixelated large format CMOS sensor for x-ray microbeam radiotherapy, Med. Phys. 47 (3) (2020) 1305–1316, http://dx.doi.org/10.1002/mp.13971.

[12] I. Sedgwick, D. Das, N. Guerrini, B. Marsh, R. Turchetta, LASSENA: A 6.7 Megapixel, 3-sides Buttable Wafer-Scale CMOS Sensor using a novel grid-addressing architecture, Proc. Int. Image Sens. Work. (2013) 3–6.

[13] F. Treibel, J.J. Wilkens, S.E. Combs, S. Bartzsch, An optimized compact microbeam source for preclinical studies, http://dx.doi.org/10.3252/pso.eu.ESTRO38.2019.

[14] S. Bartzsch, C. Cummings, S. Eismann, U. Oelfke, A preclinical microbeam facility with a conventional x-ray tube, Med. Phys. 43 (12) (2016) 6301–6308, http://dx.doi.org/10.1118/1.4966032.

[15] P. Virtanen, et al., SciPy 1.0: Fundamental Algorithms for Scientific Computing in Python, Nature Methods 17 (2020) 261–272, http://dx.doi.org/10.1038/s41592-019-0686-2.